

The motion of long bubbles in tubes

By F. P. BRETHERTON

Trinity College, Cambridge

(Received 9 November 1960)

A long bubble of a fluid of negligible viscosity is moving steadily in a tube filled with liquid of viscosity μ at small Reynolds number, the interfacial tension being σ . The angle of contact at the wall is zero. Two related problems are treated here.

In the first the tube radius r is so small that gravitational effects are negligible, and theory shows that the speed U of the bubble exceeds the average speed of the fluid in the tube by an amount UW , where

$$W \simeq 1.29(3\mu U/\sigma)^{\frac{1}{2}} \quad \text{as} \quad \mu U/\sigma \rightarrow 0.$$

(This result is in error by no more than 10% provided $\mu U/\sigma < 5 \times 10^{-3}$.) The pressure drop, P , across such a bubble is given by

$$P \simeq 3.58(3\mu U/\sigma)^{\frac{1}{2}} \sigma/r \quad \text{as} \quad \mu U/\sigma \rightarrow 0$$

and W is uniquely determined by conditions near the leading meniscus. The interface near the rear meniscus has a wave-like appearance. This provides a partial theory of the indicator bubble commonly used to measure liquid flow-rates in capillaries. A similar theory is applicable to the two-dimensional motion round a meniscus between two parallel plates. Experimental results given here for the value of W agree well neither with theory nor with previous experiments by other workers. No explanation is given for the discrepancies.

In the second problem the tube is wider, vertical, and sealed at one end. The bubble now moves under the effect of gravity, but it is shown that it will not rise at all if

$$\rho g r^2/\sigma < 0.842,$$

where ρ is the difference in density between the fluids inside and outside the bubble. If

$$0.842 < \rho g r^2/\sigma < 1.04, \quad \text{then} \quad \rho g r^2/\sigma - 0.842 \simeq 1.25(\mu U/\sigma)^{\frac{1}{2}} + 2.24(\mu U/\sigma)^{\frac{1}{3}},$$

accurate to within 10%. Experiments are adduced in support of these results, though there is disagreement with previous work.

1. Introduction

In many physical experiments the rate of flow of a liquid is measured by passing it through a capillary tube of radius r , containing an indicator bubble of air, of length several tube diameters. It was pointed out by Fairbrother & Stubbs (1935) that such a bubble moves somewhat faster than the average speed of the liquid in the tube, because it does not behave like a closely fitting piston. Motion

in which the ends of the bubble formed two hemispherical caps filling the tube cross-section would involve infinite viscous stresses at the wall. The only physical forces tending to maintain the shape of the ends against these stresses are those due to the uniform pressure within the bubble, to surface tension, and to gravity. If the tube radius is sufficiently small for gravity to be negligible, it is to be expected that there will be a film of liquid of uniform thickness b between the front and rear menisci, which is in a region of uniform pressure with no tangential stress on the free surface, and therefore at rest. Goldsmith & Mason (1960) have shown experimentally that this is indeed so. The volume swept out by the bubble when moving with speed U must equal the average speed of the liquid in front and behind it, multiplied by the cross-sectional area of the tube. This average speed is thus less than that of the bubble, in the ratio $1 - W = (1 - b/r)^2$. Measurements or calculation of the film thickness b therefore provide corresponding values for W .

The first problem considered in this paper concerns the balance between surface-tension and viscous forces for a steadily moving interface between an incompressible fluid of viscosity μ and another negligible viscosity, both being contained in a circular tube of radius r . The viscous fluid is assumed to wet the tube wall and the interfacial tension σ is assumed well defined and constant. This implies that the viscous stress tangential to the interface vanishes. The magnitudes of inertial, gravitational and viscous forces, relative to surface-tension force, are given roughly by the dimensionless numbers

$$\rho r U^2 / \sigma, \quad \rho g r^2 / \sigma, \quad \mu U / \sigma,$$

where ρ is a representative density, and U is the speed of the bubble. We shall assume to begin with that

$$\rho r U / \mu \ll 1, \quad \rho g r^2 / \sigma \ll 1.$$

The first condition is that the Reynolds number based on the tube radius is small, and the second that surface-tension forces are much more important than gravitational forces. These requirements will later be somewhat relaxed. The ratios b/r and W must then be determined by consideration of viscous and surface-tension forces alone, and so are functions only of $\mu U / \sigma$. Fairbrother & Stubbs (1935) confirmed this and suggested after several experiments that

$$W = 1.0(\mu U / \sigma)^{\frac{1}{2}} \quad \text{for} \quad \mu U / \sigma < 0.015. \quad (1)$$

These results have been extended by Taylor (1961) to values of $\mu U / \sigma$ between 0.015 and 2. Equation 1 is valid till $\mu U / \sigma$ reaches 0.09, while for larger values W asymptotes to 0.56. Marchessault & Mason (1960) have proposed the relation

$$W = (\mu / \sigma)^{\frac{1}{2}} \{ -0.10 + 1.78 / U^{\frac{1}{2}} \}$$

for $\mu U / \sigma$ between 7×10^{-6} and 2×10^{-4} . In §2 of this paper a theory is presented which leads to the result

$$W \simeq 1.29(3\mu U / \sigma)^{\frac{2}{3}}, \quad (2)$$

accurate to within 5% if $\mu U / \sigma < 0.003$. In view of the discrepancies between these values, the author repeated Fairbrother & Stubbs's experiments using a different method. The results are reported in §3.

The second problem considered (§4) concerns a wider tube, vertical and sealed at one end, so that gravity is important. On dimensional grounds the speed of rise U at low Reynolds number must be given by

$$\mu U/\sigma = f(\rho g r^2/\sigma)$$

for some function f , where ρ is now the difference in density between the fluid outside and that inside the bubble. The basic method used to determine f is similar to that of the first problem, but the results are quite different.

It was noticed by Gibson (1913) and independently by Barr (1926) that if $\rho g r^2/\sigma$ is sufficiently small the bubble does not rise at all. Barr gives a critical value of 0.15. Goldsmith & Mason (1960) suggest instead $\rho g r^2/\sigma > 1.27$ as a criterion for a rising bubble. The analysis of §4 yields $\rho g r^2/\sigma > 0.842$, and this is briefly confirmed by experiment.

The idea behind the theoretical treatment of these two problems is that for sufficiently small $\mu U/\sigma$ the viscous stresses appreciably modify the static profile of the bubble only very near the wall. In this region it turns out that the 'lubrication approximation' gives a good description of the flow and of the profile. In the centre of the tube the static profile is still appropriate and there is a region of overlap in which the two are matched. In §§2.1 and 4.1 the approximate equations are stated without derivation; §§2.2 and 4.2 the self-consistency of this process is examined retrospectively, and an estimate obtained for the range of values of $\mu U/\sigma$ for which it is valid.

2. Bubble in a capillary tube. Theory

2.1. *First approximation*

(i) In this section gravity is assumed negligible. A section of the bubble is given in figure 1 and this is assumed axisymmetric. A gross violation of this symmetry would be visible in practice and does not seem to occur. Also, in this problem, the motion near the wall is essentially determined by a local mechanism, and there is no obvious way in which the interaction between the flow at opposite ends of a diameter can arise, which is a feature of the asymmetric descent under gravity of solid spheres closely fitting in a tube, as considered by Christopherson & Dowson (1959).

For a bubble at rest there are no viscous stresses. The front and rear menisci must assume shapes of constant mean curvature κ_1 . The only such axisymmetric shape with no singularity on the axis is a portion of a sphere and, if the angle of contact at the wall is zero, it must be a hemisphere.

For sufficiently small non-zero $\mu U/\sigma$, the interface may be divided into several regions. The front and rear menisci are separated by a region CD , where a uniform film of fluid is at rest on the wall of the tube. This region is taken to be long compared to the film thickness b . The contribution to mean curvature due to axial symmetry is constant and equal to $1/(r-b)$. Also, it is assumed that $b/r \ll 1$. Away from the wall the viscous stresses are $O(\mu U/r)$, whereas stresses due to surface tension are $O(\sigma \kappa_1)$. Thus, in regions AB , EF the fractional change in mean curvature, $\delta \kappa_1/\kappa_1$, due to the motion is $O(\mu U/\sigma)$. However, in regions BC , DE

the viscous stresses are $O(\mu U/b)$ and κ_1 changes from approximately $2/r$ at B, E to approximately $1/r$ at C, D . It cannot be deduced that $b/r = O(\mu U/\sigma)$, for only gradients of stress, rather than the stresses themselves, can be equated. In the regions BC, DE variations of the viscous stress are across the film, in a distance of $O(b)$, but changes in surface-tension stress occur along the tube and may be of larger scale. It will appear later that the relevant value is $O(br)^{\frac{1}{2}}$. In the centre of the tube, however, both variations must be of the same scale $O(r)$.

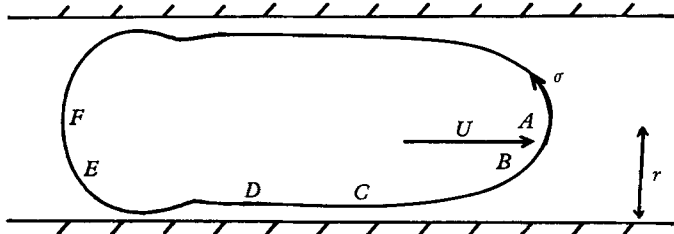


FIGURE 1. Section of a bubble in a horizontal tube.

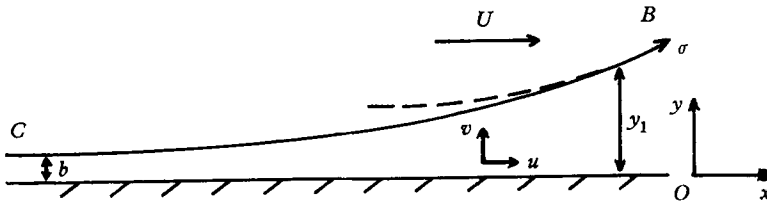


FIGURE 2. The transition region.

(ii) We now consider in detail the transition regions BC, DE using the notation of figure 2. For sufficiently small $\mu U/\sigma$ the interface, $y = y_1$, is almost parallel to the tube wall throughout the region, and the fluid thickness is much less than the tube radius, so it is plausible that the ‘lubrication approximation’ may describe the flow. Accordingly we make the following approximations.

The fluid motion in the transition region may be treated as if the region were plane, not annular. Further we take $dy/dx \ll 1$ throughout the region. The pressure p_1 within the film is effectively independent of y for given x , and the x -derivatives of velocity u_x, u_{xx} , etc., may be neglected in comparison with the corresponding y -derivatives, u_y, u_{yy} . The condition of zero tangential stress at the interface reduces to

$$u_y = 0, \quad \text{when } y = y_1, \tag{3}$$

and the normal stress condition at the interface,

$$p_1 + \sigma \kappa_1 = -2\mu\{1 + (dy_1/dx)^2\}^{\frac{1}{2}} u_x, \quad \text{when } y = y_1,$$

can be taken as

$$p_1 = -\sigma \frac{d^2 y_1}{dx^2} - \frac{\sigma}{r}. \tag{4}$$

That these approximations are self-consistent will be shown ‘a posteriori’ in §2.2.

Under these conditions, the Navier–Stokes equations for small Reynolds number become

$$u_{yy} = \frac{1}{\mu} \frac{dp_1}{dx} \quad (5)$$

and the boundary condition at the wall is

$$u = 0 \quad \text{when} \quad y = 0. \quad (6)$$

The volume-flux of fluid in unit time per unit of circumference at any value of x is

$$V = \int_0^{y_1} u \left(1 - \frac{y}{r}\right) dy,$$

or, to the approximation considered in this subsection,

$$V = \int_0^{y_1} u dy = -\frac{y_1^3}{3\mu} \frac{dp_1}{dx} \quad (7)$$

from repeated integration of equation (5), using boundary conditions (3) and (6). However, since the motion is steady continuity requires, again approximating,

$$V = U(y_1 - c), \quad (8)$$

for some constant c . Using the pressure boundary condition we obtain

$$\frac{d^3 y_1}{dx^3} = \frac{3\mu U}{\sigma} \frac{y_1 - c}{y_1}. \quad (9)$$

But when $y_1 = b$, $d^3 y_1/dx^3 = 0$, so $c = b$. Equation (9) describes the profile of the film throughout the region $BCDE$. It may be put in universal form by the substitutions

$$y_1 = b\eta, \quad x = b(3\mu U/\sigma)^{-\frac{1}{3}} \xi. \quad (10)$$

Then

$$\frac{d^3 \eta}{d\xi^3} = \frac{\eta - 1}{\eta^3}. \quad (11)$$

The author is indebted to Sir Geoffrey Taylor, who first drew his attention to this equation.

(iii) The relations (10) show that, for a given solution of equation (11) and for sufficiently small $(3\mu U/\sigma)^{\frac{1}{3}}$, there will exist regions in which

$$\eta = y/b \gg 1 \quad \text{and} \quad y_1/r = b\eta/r \ll 1,$$

but in which

$$\frac{dy_1}{dx} = \left(\frac{3\mu U}{\sigma}\right)^{\frac{1}{3}} \frac{d\eta}{d\xi} \ll 1,$$

so that equation (9) is still valid. Then from equation (11) we see that in these regions $d^3 \eta/d\xi^3 \simeq 0$ and

$$\eta \simeq \frac{1}{2} P \xi^2 + Q \xi + R,$$

for some constants P , Q , R . This gives

$$y_1 \simeq \frac{1}{2} P \left(\frac{3\mu U}{\sigma}\right)^{\frac{1}{3}} \frac{x^2}{b} + Q \left(\frac{3\mu U}{\sigma}\right)^{\frac{1}{3}} x + Rb. \quad (12)$$

However, in this region the mean curvature

$$\kappa_1 \simeq \frac{d^2 y_1}{dx^2} + \frac{1}{r} \simeq \left(\frac{3\mu U}{\sigma}\right)^{\frac{1}{3}} \frac{P}{b} + \frac{1}{r}.$$

Equation (12) thus refers to a region of constant mean curvature and thus describes a profile determined by surface tension alone. This may be extended beyond B, E outside the range of validity of equation (9), $b\eta/r \ll 1$, into the central regions AB, EF of the tube. There the previous analysis does not hold, but viscous stresses must still have a negligible influence on the profile. This is thus a surface of constant mean curvature extending across the tube with tangent nearly parallel to the wall at a distance $O(b/r)$ from it. It is therefore a portion of a sphere of radius r to a first approximation, and the mean curvature of the profile described by equation (12) is to this approximation $2/r$. Thus

$$\frac{b}{r} = \left(\frac{3\mu U}{\sigma}\right)^{\frac{2}{3}} P. \tag{13}$$

The constants P, Q, R , will not, in general, be the same at the two ends B, E . But since they refer to one solution of equation (11), continuous in the whole region $BCDE$, there are relations between their values.

In region CD , $y_1 \simeq b$ and $d^3\eta/d\xi^3 \simeq \eta - 1$. This has the general solution

$$\eta = 1 + \alpha e^\xi + \beta e^{-\frac{1}{2}\xi} \cos(\sqrt{3}\xi/2) + \gamma e^{-\frac{1}{2}\xi} \sin(\sqrt{3}\xi/2). \tag{14}$$

All terms on the right-hand side but the first are small compared to unity throughout the region CD . If $(l/b)(3\mu U/\sigma)^{\frac{2}{3}} \gg 1$ where l is the length CD , we have

$$\text{near } C, \quad \eta - 1 \simeq \alpha e^\xi, \tag{15}$$

$$\text{near } D, \quad \eta - 1 \simeq \beta e^{-\frac{1}{2}\xi} \cos(\sqrt{3}\xi/2) + \gamma e^{-\frac{1}{2}\xi} \sin(\sqrt{3}\xi/2). \tag{16}$$

These equations indicate that the front and rear menisci may be treated separately, and that there is a fundamental difference between them.

(iv) Equation (15) contains one disposable constant α , but this may be made unity by a suitable change of origin of ξ . There is near C essentially a unique solution of equation (11), and by stepwise integration in the direction of increasing ξ one obtains, relative to this origin, unique values of the constants, P, Q, R . The position of the origin is, however, physically irrelevant. We might equally choose it so that Q vanishes. A different choice yields the same profile shifted laterally, and corresponds to a bubble of the same shape in a slightly different position in the tube.

This integration has been performed for the author by Mr B. M. M. Hardisty, obtaining $P = 0.643, Q = 0, R = 2.79$, whence using equation (13)

$$b/r = 0.643(3\mu U/\sigma)^{\frac{2}{3}}. \tag{17}$$

The whole of the analysis thus far has hinged on the assumption that b/r is small. This is now seen to be self-consistent for small values of $(3\mu U/\sigma)^{\frac{2}{3}}$. A full discussion of all the approximations made will be found in §2.2.

Substituting in equation (12), near B , we have

$$y_1 = \frac{1}{2}(x^2/r) + 1.79(3\mu U/\sigma)^{\frac{2}{3}} r. \tag{18}$$

Now the right-hand side of equation (9) describes the effect of viscous forces on the curvature of the bubble interface in the region where these forces are largest, namely near the wall. The departures from sphericity in regions AB, EF , are of

the same order as the change in the curvature d^2y_1/dx^2 obtained by truncating the integration of equation (9) at the largest value of y_1 for which $dy_1/dx \ll 1$ is valid. Thus, to the approximation considered in this section, equation (18) describes in the region BC an accurate continuation of the spherical region AB . This virtual hemisphere (shown as a dashed curve in figure 2) has a tangent parallel to the wall at a distance $r\{1 - 1.79(3\mu U/\sigma)^{\frac{2}{3}}\}$ from the centre of the tube. Thus the true mean curvature of the region AB is $(2/r)\{1 + 1.79(3\mu U/\sigma)^{\frac{2}{3}}\}$. The small difference from $2/r$ does not invalidate the identification (13), but this observation does enable us to estimate the pressure drop across a moving front meniscus. This arises partly from viscous stresses in the Poiseuille flow in the capillary and in the unknown motion near the central spherical portion of the meniscus, and partly from the pressure drop across the interface itself, due to surface tension forces. For any given geometrical arrangement, the viscous stresses are proportional to $\mu U/r$, whereas the surface tension stresses are

$$(2\sigma/r)\{1 + 1.79(3\mu U/\sigma)^{\frac{2}{3}}\}.$$

Thus the dynamic pressure drop $3.58(3\mu U/\sigma)^{\frac{2}{3}}(\sigma/r)$ will dominate for sufficiently small $(\mu U/\sigma)$.

(v) At the rear meniscus the situation is different. In equation (16) are two disposable constants. Change of origin in ξ , which corresponds to lateral displacement of the whole rear meniscus without change of shape, can account for one of these, but it is still possible, by varying the other, to obtain by stepwise integration any value of $P \geq 0$ and corresponding values of Q, R . Thus the identification (13) may be carried through for any value of b/r . Given b/r , however, there corresponds a unique profile and a well-defined virtual hemisphere. The profiles all show oscillations in thickness, the minimum value of y/b decreasing as P increases. The pressure drop across a moving rear meniscus exceeds the static value $2\sigma/r$ only if $(b/r)(3\mu U/\sigma)^{-\frac{2}{3}} < 0.9$. For larger values it tends to assist rather than hinder the motion. The necessary energy comes from the finite volume of liquid in the film of thickness b at a pressure σ/r higher than the liquid behind the meniscus. For values of $(b/r)(3\mu U/\sigma)^{-\frac{2}{3}} < 0.9$ the energy dissipated in the transition region DE exceeds this amount and external work has to be done to make the meniscus move. If b/r is defined by a front meniscus travelling with the same speed U , $(b/r)(3\mu U/\sigma)^{-\frac{2}{3}} = 0.643$, the dynamic pressure drop is found to be $-0.930(3\mu U/\sigma)^{\frac{2}{3}}\sigma/r$, and the minimum film thickness to be $0.716b$. Thus the rear meniscus contributes to the total dynamic pressure drop across the bubble, which is $4.52(\sigma/r)(3\mu U/\sigma)^{\frac{2}{3}}$.

(vi) It remains to calculate the value of W , the fractional velocity correction measured by Fairbrother & Stubbs. This is easily seen to be the proportion of the cross-sectional area of the tube occupied by the film of thickness b , so

$$W = 1.29(3\mu U/\sigma)^{\frac{2}{3}} \quad (19)$$

to the approximation considered here.

(vii) A meniscus at rest between two parallel plates in such a way that the radius of curvature in the plane of the plates is large compared to the distance between them must assume an almost semicircular profile when viewed in normal

section in a plane at right angles to the plates. Changes in curvature due to symmetry about the tube axis do not enter into equation (9), so the theory of this subsection can be taken over directly to the almost two-dimensional motion about a moving meniscus between two parallel plates. The only amendment is that the pressure drop across each meniscus should be halved.

2.2. Justification of the approximations

In this subsection we review and extend the approximations made in §2.1. These arise in several different ways and will be treated separately.

(i) Consider first the requirement that inertia forces can be neglected in comparison with viscous forces. The previous analysis shows that, provided inertia forces are not so large as to cause appreciable distortion near the centre, this is important only near the walls where the interface profile departs appreciably from the spherical. In nearly parallel flow the appropriate Reynolds number measuring the relative importance of inertial and viscous forces is $\rho Ub^2/\mu L$, where L is the length scale of variations downstream, in this case $r(\mu U/\sigma)^{\frac{1}{2}}$. To neglect inertia we require not $\rho Ur/\mu \ll 1$, but

$$\rho r U^2/\sigma \ll 1.$$

This is also the condition that inertia forces are negligible in the centre of the tube.

(ii) Secondly, consider the neglect of gravity forces. These can be important both in affecting the flow in the film remaining on the wall, and also in distorting the shape of a static meniscus which we have assumed spherical. The first will not affect the proportion of fluid left behind by the front meniscus; such fluid will merely drain to the lowest generator of the tube. The time scale for this is much longer than the time taken for the meniscus to move a tube diameter if $\rho gb^2/\mu U \ll 1$, i.e. if

$$(\rho gr^2/\sigma)(\mu U/\sigma)^{\frac{1}{2}} \ll 1.$$

The change in static profile affects the identification (13). If $\rho gr^2/\sigma$ is appreciable, κ_1 varies from point to point of region AB . Thus $(3\mu U/\sigma)^{\frac{1}{2}}(P/b)$ will also vary, and the average value of b over the tube circumference might differ from that given by equation (13). The complete solution of this problem for a horizontal tube is difficult. It is that of finding the surface which touches the wall of a horizontal cylinder, and which has a curvature linearly dependent on the height above the lowest generator. The relevant non-linear partial differential equation has no obvious general solution. However, the author has assumed $(\rho gr^2/\sigma)^2$ to be negligible and obtained the resultant small perturbations of the surface from a hemisphere. To this approximation, the average value of b/r for a horizontal tube is identical with that given by equation (13).

For a vertical tube the problem is easier. The ratio b/r is increased by a factor $1 + \frac{2}{3}\rho gr^2/\sigma + O(\rho gr^2/\sigma)^2$ for a rising bubble and by $1 - (\frac{2}{3}\rho gr^2/\sigma) + O(\rho gr^2/\sigma)^2$ for a descending one.

(iii) The last and most significant approximations are those made to obtain a solution of the problem in which gravity and inertia are entirely neglected. The value of b/r obtained, which is $O(\mu U/\sigma)^{\frac{1}{2}}$, shows that the contribution of the axial

symmetry to the mean curvature of the interface in the transition regions differs from $1/r$ by an amount of order $(1/r)(\mu U/\sigma)^{\frac{1}{2}}$. The neglect of this in equation (9) is justified, for d^2y_1/dx^2 is of order $1/r$. For similar reasons terms like $2\mu u_x$ in the pressure-boundary condition and corrections to the equations of continuity are all found, when calculated, to be negligible provided $(\mu U/\sigma)^{\frac{1}{2}}$ is sufficiently small. Just how small 'sufficiently' is will be established in the remainder of this subsection, which is devoted to setting up the exact equations and using the results of §2.1 to obtain a closer approximation. Thence the range of validity of these results will become apparent.

(iv) We use the notation of figure 2, remembering that the flow is axisymmetric. Neglecting inertia terms the Navier-Stokes equations become

$$\begin{aligned}\frac{1}{\mu}p_x &= u_{xx} + u_{yy} - \frac{1}{r-y}u_y, \\ \frac{1}{\mu}p_y &= v_{xx} + v_{yy} - \frac{1}{r-y}v_y - \frac{1}{(r-y)^2}v.\end{aligned}\quad (20)$$

The equation of continuity is

$$u_x + v_y - \frac{v}{r-y} = 0, \quad (21)$$

and the boundary conditions at the wall are

$$u = v = 0, \quad \text{when } y = 0. \quad (22)$$

At the surface $y = y_1$, the normal has direction cosines $(-\sin\theta, \cos\theta)$ where $\tan\theta = dy_1/dx$. The components of the stress tensor are

$$p_{xx}: -p + 2\mu u_x; \quad p_{yy}: -p + 2\mu u_y; \quad p_{xy}: \mu(u_y + v_x).$$

We equate the tangential and normal stresses to 0 and $\sigma\kappa_1$ respectively, giving

$$\begin{aligned}\mu\{(u_x - v_y)(-2\sin\theta\cos\theta) + (u_y + v_x)(\cos^2\theta - \sin^2\theta)\} &= 0, \\ -p + \mu\{2u_x\sin^2\theta + 2v_y\cos^2\theta - 2(u_y + v_x)\sin\theta\cos\theta\} &= \sigma\kappa_1.\end{aligned}$$

At this stage it is an advantage to develop the notation. The suffix 1 attached to any symbol denotes that its value is to be taken on the surface $y = y_1$. The prime ' denotes differentiation with respect to x along the surface. We must distinguish carefully between, for example, u_{x1} and u'_1 . The former is the value of $\partial u/\partial x$ taken at $y = y_1$; the latter is the derivative of the value of u at the free surface, and is $u_{x1} + u_{y1}y'_1$. Remembering that $\tan\theta = y'_1$ and using equation (21), after some manipulation the surface-boundary conditions may be written

$$u_{y1} = -v_{x1} + \left(2u_{x1} - \frac{v_1}{r-y_1}\right) \frac{2y'_1}{1-y_1'^2} \quad (23)$$

$$\text{and} \quad -\sigma\kappa_1 - p_1 = \left(2u_{x1} - \frac{v_1}{r-y_1}\right) (1+y_1'^2)^{\frac{1}{2}} - \frac{v_1}{r-y_1}, \quad (24)$$

$$\text{where} \quad \kappa_1 - y_1'' = y_1''\{(1+y_1'^2)^{-\frac{3}{2}} - 1\} + (1+y_1'^2)^{-\frac{1}{2}}/r - y_1. \quad (25)$$

The Navier–Stokes equations become

$$u_{yy} - \frac{1}{\mu} p_1' = -u_{xx} + \frac{u_y}{r-y} + \frac{1}{\mu} (p_x - p_1'), \quad (26)$$

and the continuity conditions

$$V - \int_0^{y_1} u \, dy = - \int_0^{y_1} u \frac{y}{r} \, dy \quad (27)$$

and

$$V - U(y_1 - c) = -U y_1^2 / 2r \quad (28)$$

complete the exact equations for this problem. We see that in the previous subsection everything on the right-hand side of these equations was neglected. Neglecting these small terms, triple integration of equation (26) with respect to y using boundary conditions (22), (23) and substitution in equation (27) gave an expression for V , equation (7).

We now repeat this procedure—but retaining the neglected terms. Thus,

$$\begin{aligned} V + \frac{y_1^3}{3\mu} p_1' &= \int_0^{y_1} dy \int_0^y dy \int_{y_1}^y \left\{ \frac{1}{\mu} (p_x - p_1') - u_{xx} + \frac{u_y}{r-y} \right\} dy \\ &\quad + \frac{y_1^2}{2} \left\{ -v_{x1} + \left(2u_{x1} - \frac{v_1}{r-y_1} \right) \frac{2y_1'}{1-y_1'^2} \right\} - \int_0^{y_1} u \frac{y}{r} \, dy. \end{aligned} \quad (29)$$

We now manipulate these integrals until they involve solely integrations with respect to y of the x -derivatives of u , y_1 . This may always be done, for, from equation (21)

$$v = \frac{1}{r-y} \int_0^y -u_x(r-y) \, dy$$

and

$$\begin{aligned} \frac{1}{\mu} (p_x - p_1') &= \frac{\partial}{\partial x} \left\{ \int_{y_1}^y \frac{1}{\mu} p_y \, dy \right\} \\ &= \frac{\partial}{\partial x} \left\{ \int_{y_1}^y dy \left[v_{xx} + v_{yy} - \frac{1}{r-y} \left(v_y + \frac{v}{r-y} \right) \right] \right\}. \end{aligned}$$

The analysis so far is exact. But these integrals are of an order smaller by $(\mu U/\sigma)^{\frac{2}{3}}$ than the terms on the left-hand side of equation (29). For they all involve either x -derivatives to at least second order or products of first order, or a factor y_1/r , and in the last subsection $y_1' = O(\mu U/\sigma)^{\frac{1}{3}}$, and $y_1/r = O(\mu U/\sigma)^{\frac{2}{3}}$. Thus, if we use the values of u obtained in the last subsection by integration of equation (5) to evaluate these integrals, we will obtain an approximation valid to $(\mu U/\sigma)^{\frac{2}{3}}$ higher order.

$$V + \frac{y_1^3}{3\mu} p_1' = -\frac{4}{15\mu} y_1^3 p_1''' - \frac{5}{3\mu} y_1^4 y_1' p_1'' - \frac{1}{3\mu} y_1^3 (y_1 y_1'' + 5y_1'^2) p_1' + \frac{1}{3\mu r} y_1^4 p_1'.$$

Using now equations (7), (8) to the same approximation

$$p_1' + 3\mu U \frac{y_1 - c}{y_1^3} = -\frac{3\mu U}{y_1^3} \left\{ \frac{3y_1 - 7c}{5} y_1 y_1'' + \frac{y_1 - 2c}{5} y_1'^2 + \frac{y_1}{2r} (y_1 - 2c) \right\}. \quad (30)$$

Up to this stage we have not used the condition (24) on the normal stress on the interface. Equation (30) is derived only from the equations of motion and

continuity and from the absence of tangential stress. The value of the constant c becomes clear when we substitute for the pressure. To the same approximation then

$$\kappa_1' - \frac{3\mu U}{\sigma} \frac{y_1 - c}{y_1^3} = \frac{3\mu U}{\sigma} \frac{1}{y_1^3} \left\{ \frac{3}{5} y_1 y_1''(y_1 + 4c) + \frac{1}{5} y_1'^2(y_1 + 8c) + \frac{y_1}{2r}(y_1 - 2c) \right\}. \quad (31)$$

When $y_1 = b$, $y_1' = y_1'' = 0$, $\kappa_1 = 1/(r - b)$, so we have $b - c = -b(b - 2c)/2r$, i.e.

$$c \simeq b - (b^2/2r).$$

Finally, it should be noted that the exact form of equation (19) expressing W in terms of b is

$$W = \frac{2b}{r} \left(1 - \frac{b}{2r} \right). \quad (32)$$

(v) Equation (31) is the next approximation to equation (9). It is convenient to leave the mean curvature κ_1 in its exact form, equation (25), but otherwise

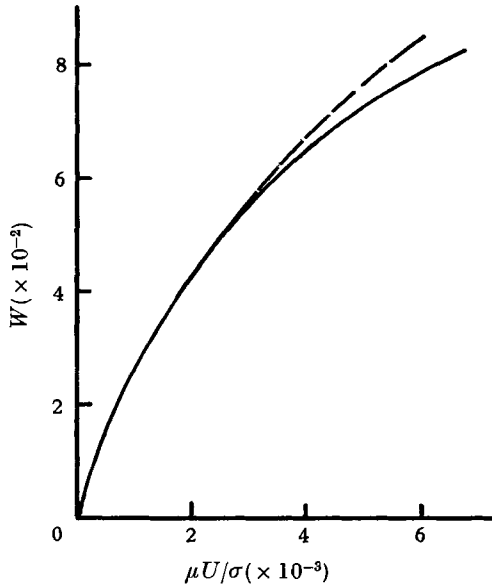


FIGURE 3. The correction W as a function of $\mu U/\sigma$. ——— $1.29(3\mu U/\sigma)^{1/2}$; ——— solutions of equation (31).

the only difference is the addition of the terms on the right-hand side. These are all $O(3\mu U/\sigma)^{1/2}$ smaller than those on the left, and it is apparent too, that they are uniformly smaller, except when y_1/b becomes large. When y_1/b becomes large, but y_1/r is still small, the value of κ_1' approaches zero and the profile is approximately a surface of constant mean curvature. As y_1/r increases further κ_1' increases again, and equation (31) is clearly invalid. If, however, $(3\mu U/\sigma)^{1/2}$ is sufficiently small the minimum value of κ_1' can be made arbitrarily near zero, and the matching of the profile at that point to a portion of a sphere extending across the central portions of the tube may be made arbitrarily good. Thus, with the boundary conditions that $y_1 \rightarrow b$ as $x \rightarrow -\infty$, and that, for large y_1/b , y_1, y_1', y_1''

should be matched to those values appropriate to a spherical region of some curvature centred on $y_1 = r$, equation (31) apparently comprises the first two terms of an asymptotic expansion in powers of $(3\mu U/\sigma)^{\frac{1}{2}}$ of the exact equation describing the profile. It could in principle be used as the basis for obtaining still higher approximations by the same method. The solution of equation (31) presumably provides the first two terms of an asymptotic expansion of the profile itself.

(vi) Solutions of equation (31) have been obtained numerically using a digital computer. The results are shown in figure 3. For values of $\mu U/\sigma$ larger than 5×10^{-3} it was clear from the solutions that the minimum value of κ'_1 , attained for large values of y_1/b before the terms in $y_1'^2/y_1^2$ on the right-hand side became large again, was insufficiently small for an accurate match to a sphere to be made. This implies that further terms in the asymptotic expansion must be taken for larger values of $\mu U/\sigma$.

(vii) To summarize the results of this subsection: The range of values of $\mu U/\sigma$ for which the calculated values of W are likely to be accurate and yet are appreciably different from the two-thirds power law of § 2.2 is quite small, so the main value of the calculations of the subsection is to delimit accurately the upper limit to the range of validity of that law. It is accurate to within 5%, at $\mu U/\sigma = 3 \times 10^{-3}$. Neglect of inertia forces is permissible if $\rho r U^2/\sigma \ll 1$. The effect of gravity on a horizontal tube is $O(\rho g r^2/\sigma)^2$ but first order in $\rho g r^2/\sigma$ for other orientations.

3. Bubble in a capillary tube. Experiments

3.1. Method and results

Fairbrother & Stubbs estimated directly the fractional correction W to the speed of a bubble by measuring the volume of fluid ejected from the tube when the bubble moved a known distance. This method requires an accurate knowledge of the tube radius, and the final correction is obtained from the small difference between two volumes measured in different ways. To avoid gravitational effects the tube diameter must be small, yet if it is too small estimation of volumes becomes difficult. Their experiments were confined, for this reason, to tubes of 2 mm diameter. Their experiments extend down to $\mu U/\sigma = 1 \times 10^{-4}$. Marchessault & Mason (1960) derived the film thickness from the electrical resistance of the tube containing a bubble of known length. Their values for W , mainly for smaller $\mu U/\sigma$, are all somewhat larger than those calculated from the Fairbrother & Stubbs formula. In view of the clear discrepancy between this work and the prediction of this paper (equation 2) the author has repeated these experiments using a different method. Values of W for two different fluids in a 1 mm tube are given in figure 4. The dependence of these curves on the fluid used shows that the physical assumptions made in § 2 are inadequate, but the author is unable to postulate any reason which could, even qualitatively, explain the divergences between different fluids and from the theory.

Because of this it is proposed to give a detailed account of the experimental technique used here and then to conclude with a negative discussion of the causes of the discrepancy.

The apparatus used is shown in figure 5. A column of fluid LM , a few centimetres long, was drawn at constant rate about 100 cm along a carefully cleaned and dried 'Veridia' glass tube of 1 mm diameter. This was achieved by coupling the flow to that of a constant head of viscous oil (Shell Diala) across lengths of hypodermic tubing (providing a higher resistance than the 'Veridia' glass tube).

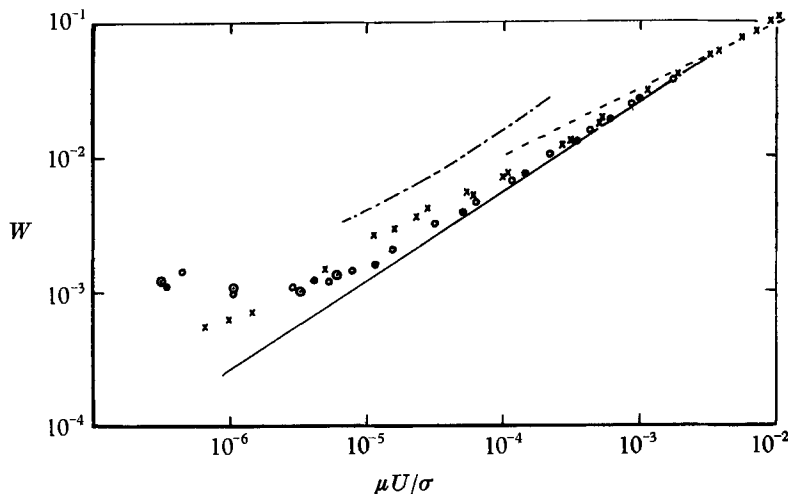


FIGURE 4. — Theory; - - - Marchessault & Mason; - · - Fairbrother & Stubbs; × aniline, ○ benzene (horizontal tube), ⊙ benzene (with evaporation precautions), ● benzene (vertical tube).

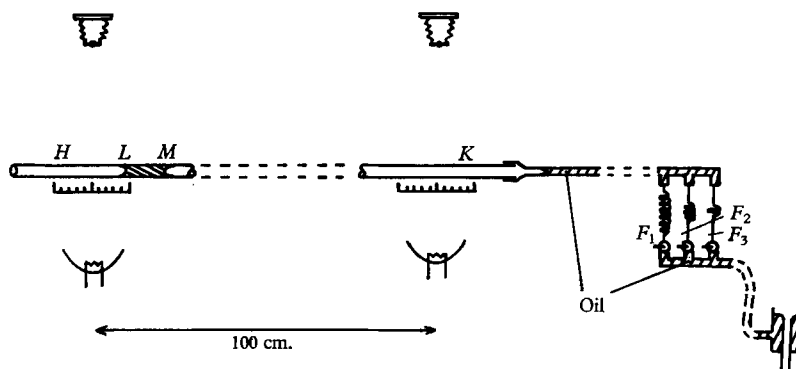


FIGURE 5. The apparatus.

Three such lengths were available, controlled by taps, F_1 , F_2 , F_3 , giving speed ratios for a given head of 50:1. The head could be supplemented, if necessary, using mercury, up to a maximum of 20 cm Hg. Near the points H , K flash photographs of the column gave measurements of its length accurate to ± 0.001 cm. The average speed U of the rear meniscus of the column was obtained, from the time interval between the flashes, to within 2% for the fastest run (9.5 sec). The change in length of the column, divided by the length of run, gives the proportion W of fluid left behind.

The advantages of this method are several. It gives a very sensitive method of measuring the very thin film thicknesses involved, down to 2×10^{-5} cm, at which value the probable error is about 6%. This is independent of the radius of the tube, which, though it should be reasonably constant, need not be accurately known. It may also be used for volatile liquids, provided precautions are taken to saturate the air in the tube. Cleanliness is, however, vital, as a small sample of fluid is involved which touches large areas of tube wall. The apparatus was arranged so that the fluid touched no surface but glass, all of which was cleaned between every run with chromic acid, washed with distilled water, and dried using either acetone and air or by drawing filtered air through a desiccator. This is tedious but effective, and the self-consistency of the results would be improbable in the presence of significant contaminants. Indeed, this is probably the reason for the greater spread of the results for aniline. A check on the diameter of the tube and the accuracy of the length measurements was made by measuring the change in length of a column of mercury in runs in both directions. It returned exactly to its original length, showing that none had been left behind on the wall, but showed that the tube was conical with a change in tube radius of around 1%. A correction for this (never exceeding 30%) was applied to the measurements of change in length. W proved to be independent of the length of the columns used, though this was always greater than 4 tube diameters. The speed U varied during the very long runs (up to 36 h) by up to 20%, because of changes of the viscosity of Diala with room temperature. However, the mean speed was always measured, and the values of μ/σ for the estimated mean temperature obtained from tables.

Finally, the tube was mounted vertically and the same measurements made using benzene. According to §2.2 the values of W so obtained should be larger by the factor $1 + \frac{2}{3}\rho g r^2/\sigma$ than the corresponding values for a horizontal tube, provided $(\rho g r^2/\sigma)^2$ can be neglected. For benzene $\rho g r^2/\sigma$ is 0.06, so the values of W have been reduced by 4% before plotting in figure 4 to make them strictly comparable with the data from the horizontal tube.

3.2. Discussion

The results plotted in figure 4 show serious systematic divergences between theory and experiment. These are largest at the slowest speeds, whereas agreement is quite good at the upper end of the range of validity of the theory. Aniline was one of the liquids used by Fairbrother & Stubbs (1935), but their curve lies well outside the spread of points corresponding to aniline in the present measurements. There is no obvious reason for this, though in principle the method used here is probably more accurate for small values of W .

The parameter $\rho r U^2/\sigma$, which was shown in §2.2 to measure the importance of inertia, was never more than 0.1 for either fluid, and, in any case, the main discrepancies occur at much lower speeds and cannot be due to inertia effects. It might be thought that with benzene evaporation could account for the large change in volume of the column at low speeds. This is not so, as was shown by carefully saturating the air in the tube with benzene vapour. No significant difference appeared in the results. The excellent agreement between values for

the horizontal tube and the corrected ones for the vertical tube shows that gravity is satisfactorily accounted for.

The effect was at first thought to be possibly due to roughness of the inside of the tube. Hillocks and hollows of the order of 1μ in height would cause a film to be left behind which was thicker by a constant amount from that predicted by theory, and we would expect W to tend to a constant value for sufficiently small $\mu U/\sigma$, corresponding to all the hollows being full. This does not happen for aniline, and anyhow this hypotheses would not explain the differences for different fluids.

An instability of the meniscus at the lowest speeds would also presumably be a function of $\mu U/\sigma$, and in any case there is no trace of it occurring though it would be difficult to observe visually. It is also difficult to see how a lack of perfect wetting would result in more fluid being left behind at the slower speeds.

It is possible that dissolved impurities or surface charges were present which cause a 'hardening' of the free surface similar to the effect observed in the free rise of small bubbles in large volumes of fluid. These cannot be present in the quantity required to reduce the surface tension by a factor of 4 which varies systematically with time. However, they might conceivably result in the free surface in the transitional region being able to support a tangential stress, and thus make equation (9) invalid. A discussion of various mechanisms which cause 'hardening' has been given by Frumkin & Levich (1947), but it is sufficient here to consider two extreme cases.

If the free surface behaves like a rigid one throughout the transitional region, we may easily obtain the analogue of equation (9). If $b/r \ll 1$ we may neglect the change in surface tension with x from its equilibrium value, but we must replace equation (3) by

$$u = U \quad \text{when} \quad y = y_1.$$

The equation governing the profile then becomes

$$\frac{d^3 y_1}{dx^3} = \frac{6\mu U}{\sigma} \frac{y_1 - 2c}{y_1^3}. \quad (33)$$

If we make this dimensionless by

$$y_1 = 2c\eta,$$

$$x = 2c(6\mu U/\sigma)^{-1/3}\xi,$$

we see that

$$2c/a = 2^{2/3} 0.643 (3\mu U/\sigma)^{1/3}.$$

When we remember that the quantity actually measured in these experiments was c/a we see that this hypothesis of complete absence of slip actually reduces the value of W by a factor $2^{-1/3}$.

However, if we do not require that equation (33) should hold over effectively the whole transition region, it is possible to obtain an increased value of W . If equation (9) (no tangential stress) holds for $c \leq y_1 \leq e$ for some e and equation (33) for larger values, the maximum value of P we can obtain is about 0.69 for $e = 3c$, corresponding to an increase of W of only 8%. Hardening of the surface is thus quite unable to account for the observed results, and they remain a mystery to the author.

The referee has suggested that the discrepancy may be due to the 'disjoining pressure' in thin films of liquid in contact with a solid surface (Frenkel, 1946). A repulsive pressure $f(y_1)$ due to the cohesive forces between molecules appears between the surfaces of all liquid films of small thickness y_1 , and f is of order 10^3 dynes/cm² when y_1 is 0.1μ . It falls off very rapidly with film thickness, according to an inverse cube or inverse fourth power law. The corrected form of equation (9) is

$$\frac{d^3y_1}{dx^3} + \frac{1}{\sigma} \frac{df}{dy_1} \frac{dy_1}{dx} = \frac{3\mu U}{\sigma} \frac{y_1 - c}{y_1^3}.$$

The correction is negligible everywhere if $y_1(df/dy_1) \ll \sigma/r$ in the transition region. These terms are comparable in magnitude when $b = 0.25\mu$, corresponding to $W = 1 \times 10^{-3}$, but the disjoining pressure must be quite negligible when W is an order of magnitude larger. However, when $\mu U/\sigma$ is around 2×10^{-4} systematic divergences between theory and experiment, though smaller, are still apparent, particularly in the case of aniline. Thus though discrepancies at the slowest speeds may possibly be accounted for in this way, this explanation is incomplete.

4. Bubble in a vertical tube

4.1. Theory. First approximation

(i) In this section we consider the motion at low Reynolds number of a long bubble in a vertical tube sealed at one end. Gravitation enters into the problem only as a buoyancy force, and always occurs in the equations multiplied by the density difference ρ between the fluid outside and that inside the bubble. When the problem was first attempted it was thought that $\mu U/\sigma$ and $\rho g r^2/\sigma$ should tend to zero together, but the method of §2 produced nonsensical results. Observation of rising bubbles at once suggested the answer, that there is a critical value of $\rho g r^2/\sigma$ below which no rise at all takes place, and application of the lubrication assumptions to flow under small values of $\mu U/\sigma$ and values of $\rho g r^2/\sigma$ slightly greater than the critical gave self-consistent results. This application is given in the remainder of this subsection, together with reasons why no similar theory exists when ρ is slightly subcritical. In §4.2 the range of validity of the theory is considered, and finally in §4.3 some experimental confirmation is mentioned.

(ii) The method of analysis is very similar to that of the previous section. The restriction to cases when the steady speed of rise U is such that $\mu U/\sigma \ll 1$ again implies that the effect of viscous forces on the profile of the bubble will be confined to a region near the wall. Further, in the absence of contrary evidence, axial symmetry will be assumed.

The front and rear menisci are separated by the region CD (figure 6), where a uniform film of fluid is draining under the effects of gravity alone. In regions AB , EF the viscous stresses exert a negligible influence on the film profile, which is determined by static equilibrium between surface tension and gravitational stresses. In the transition regions viscous stresses are important, but the film profiles are everywhere nearly parallel to the tube wall, and the 'lubrication hypothesis' proves to be a self-consistent approximation.

(iii) In the regions AB , EF the profile is determined by the condition

$$\sigma \kappa_1 = \rho g x, \quad (34)$$

where κ_1 is the mean curvature of the surface and x the height above some fixed level. This is the equation which was treated by Bashforth & Adams (1883) in their computations on the profiles on pendent and sessile drops, and into whose results more detail has been interpolated by Fordham (1948). However, for the purpose of this paper the author required a criterion which could not be obtained

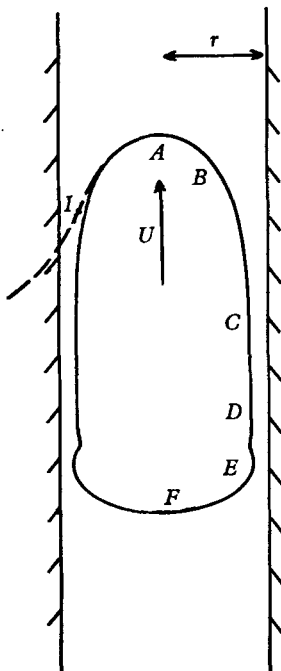


FIGURE 6. Section of a bubble in a vertical tube.

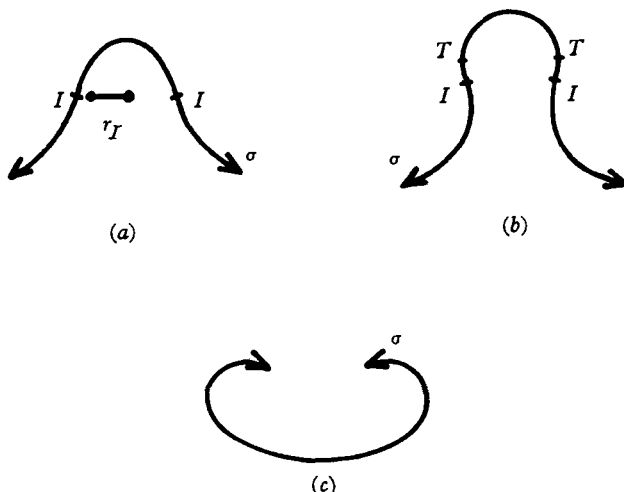


FIGURE 7. Equilibrium profiles under surface tension and gravity forces. (a) Top meniscus $\rho gr_1^2/\sigma > 0.842$; (b) top meniscus $\rho gr_1^2/\sigma < 0.842$; (c) bottom meniscus.

accurately from these tables, so the digital computer EDSAC II was programmed to give it. The calculated profiles for region AB may be divided into two classes shown diagrammatically in figure 7 (a) and (b). A member of each of these has a point of inflexion I , at which the radius is r_I , but if $\rho gr_1^2/\sigma > 0.842$, as in figure 7 (a), there is no point at which the tangent plane is vertical. In figure 7 (b) the tangent plane is vertical at a point T . Furthermore, for $|(\rho gr_1^2/\sigma) - 0.842| < 0.2$, the angle ϕ made with the vertical by the tangent plane at I is given by

$$\phi = 0.49\{(\rho gr_1^2/\sigma) - 0.842\}. \quad (35)$$

The profile within this range will prove of most interest to us in the following discussion. The profiles for region EF exhibit no point of inflexion, as shown in figure 7 (c).

(iv) We now consider the transitional and uniform regions $BCDE$, using the notation of figure 8. If the rate of rise is sufficiently small, the lubrication approximations will describe the flow, and the analysis proceeds exactly as in §2, except that the pressure everywhere must be modified to account for the gravitational body force, by addition of a term ρgx . Also, the flux V_b in the uniform region is not

zero, but $\rho gb^3/3\mu$ per unit circumference. It is to be expected that, for sufficiently small $\mu U/\sigma$ the ratio of film thickness to tube radius will also be small. This proves to be self-consistent. Equation (9) of § 2.1 is modified to read

$$y_1''' - \frac{\rho g}{\sigma} = \frac{3\mu U}{\sigma} \frac{1}{y_1^3} \left(y_1 - b - \frac{\rho gb^3}{3\mu U} \right). \quad (36)$$

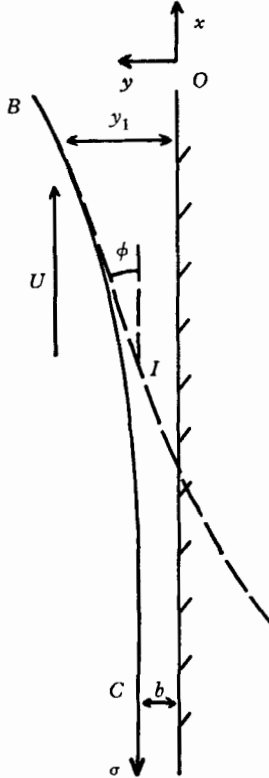


FIGURE 8. The top transition region.

In this problem, however, there is an additional continuity requirement, that all the fluid displaced by the top meniscus of the rising bubble should flow through the uniform region CD to the lower meniscus. Thus

$$-\frac{\rho gb^3}{3\mu} = V_b = -\frac{1}{2\pi r} \{U\pi(r-b)^2\},$$

i.e.
$$\frac{\rho gb^2}{3\mu U} \approx \frac{r}{2b}, \quad (37)$$

to this order of approximation. Thus, for sufficiently small b/r the last term on the right-hand side of equation (36) greatly exceeds the other two throughout region $BCDE$, and the film profile is given by

$$y_1''' = \frac{\rho g}{\sigma} \left(1 - \frac{b^3}{y_1^3} \right). \quad (38)$$

This may be made dimensionless by the substitution

$$y_1 = b\eta, \quad x = b(\rho gb^2/\sigma)^{-\frac{1}{2}}\xi, \quad (39)$$

to give
$$\eta''' = \frac{\eta^3 - 1}{\eta^3}. \quad (40)$$

(v) This equation should be compared with equation (11) of §2.1. In the region CD , $y_1 \simeq b$, $\eta''' \simeq 3(\eta - 1)$. As before this enables us to say that, given b , for a top meniscus there is an essentially unique profile, whereas for a bottom meniscus an infinite family. Also, the relations (39) show that for sufficiently small $\rho gb^2/\sigma$, provided b/r is also small, there exist regions in which

$$\eta = y_1/b \ll 1, \quad y_1/r = b\eta/r \ll 1,$$

and yet

$$y_1' = (\rho gb^2/\sigma)^{\frac{1}{2}}\eta \ll 1.$$

Here equation (38) is still valid, but $\eta''' \simeq 1$ and

$$\eta \simeq \frac{1}{3}\xi^3 + \frac{1}{2}P\xi^2 + Q\xi + R \quad (41)$$

for some constants P, Q, R , which are determined to within a change of origin at a top meniscus. However, in this region $d\kappa_1/dx \simeq y_1''' \simeq \rho g/\sigma$, so equation (41) refers to a region of equilibrium between surface tension and gravity. This is the defining condition of regions AB, EF so the profile there must be identical with that part of one of the profiles shown in figure 7 where the tangent plane is nearly vertical.

But, for a top meniscus, it can fairly easily be shown, and numerical integration confirms, that equation (31) admits of no point where $\eta' = 0$ and the tangent plane is accurately vertical. Thus, no matching at all is possible to a profile of type 7(b). For a profile of type 7(a) matching is possible within the assumptions of this section, provided ϕ is small—in other words, provided $\rho gr_1^2/\sigma$ is only slightly greater than 0.842. With origin chosen so that $P = 0$, numerical integration for a top meniscus gives

$$P = 0, \quad Q = 0.572, \quad R = 1.10.$$

At the point of inflexion I

$$y_1 = 1.10b, \quad y_1' = 0.572(\rho gb^2/\sigma)^{\frac{1}{2}}, \quad r_I = r - y_1.$$

Insertion in equations (35), (37) gives

$$\begin{aligned} \frac{\rho gr^2}{\sigma} - 0.842 &= 1.10 \left(\frac{b}{r}\right)^{\frac{3}{2}} + 1.85 \frac{b}{r} \\ &= 1.25 \left(\frac{\mu U}{\sigma}\right)^{\frac{3}{2}} + 2.24 \left(\frac{\mu U}{\sigma}\right)^{\frac{1}{2}}. \end{aligned} \quad (42)$$

Near the rear meniscus the film thickness again has a wave-like appearance and a profile can be found matching a meniscus moving with speed U to any small film thickness b .

(iv) The impossibility of matching solutions of equation (38) to a profile of type 7(a) does not demonstrate that a bubble will not rise in a tube with $\rho gr^2/\sigma < 0.842$, for it could do so unsteadily, or under conditions in which the lubrication

approximations do not hold. However, it does indicate a critical radius at which the type of flow changes drastically, and quite simple experiments are sufficient to indicate the nature of the change. These are mentioned in § 4.3.

4.2. Review of approximations

(i) The importance of inertia forces in the transition region is measured by the ratio $\rho ub^2/\mu L$, where u is a typical velocity, and L the length scale of variation along the streamlines. This latter is $b(\rho gb^2/\sigma)^{-\frac{1}{2}}$, so from continuity the relevant Reynolds number is $(\rho ur/\mu)(\rho gb^2/\sigma)^{\frac{1}{2}}$. For water this becomes of order unity when $\mu u/\sigma$ is around 8×10^{-5} , and $(\rho gr^2/\sigma) - 0.842 \simeq 0.25$, and the neglect of inertia forces is a severe limitation. However, also of importance are the geometrical and related approximations made in deriving equation (42).

(ii) To obtain an estimate of the validity of these results we note that the analysis of § 2.2 leading to equation (31) applies directly to this problem, provided we add a 'virtual pressure' ρgx to the true pressure everywhere to account for the gravitational body force. For provided the Reynolds number is small the boundary conditions and equations of motion are otherwise unaltered. Equation (31) now becomes

$$\kappa'_1 - \frac{\rho g}{\sigma} - \frac{3\mu U}{\sigma} \frac{y_1 - c}{y_1^3} = \frac{3\mu U}{\sigma} \frac{1}{y_1^3} \left\{ \frac{3}{8} y_1 y_1'' (y_1 + 4c) + \frac{1}{8} y_1'^2 (y_1 + 8c) + \frac{y_1^2 - 2cy_1}{2r} \right\}. \quad (43)$$

When $y_1 = b$, $y_1' = y_1'' = 0$, $\kappa_1 = 1/(r - b)$, so

$$\frac{\rho gb^3}{3\mu U} + b - c = -\frac{b^2 - 2bc}{2r}.$$

It is also clear from the definition of the constant c of equation (28) that if the bubble surface were to fill completely the cross-section of the tube ($y_1 = 0$) there would have to be an upward flux $-2\pi r U c$ flowing somehow past the bubble. But in this case the tube is sealed at one end, so $c = \frac{1}{2}r$ exactly. Thus the next approximation to equation (37) is

$$\frac{r}{2} = \frac{\rho gb^3}{3\mu U} + \frac{b}{2}.$$

(iii) Comparison of these equations with equations (37), (38) show that the approximations made in deriving equation (42) have arisen in three ways. The flow in the transition region is not quite unidirectional and the terms describing departures from the parabolic velocity profile are the first two on the right-hand side of equation (42), and are smaller than those retained in equation (38) by $O(b/r)^{\frac{3}{2}}$. Terms arising from the film thickness in the transition region being a finite proportion of the radius of the tube are $O(b/r)^{\frac{1}{2}}$. Finally, the neglect of changes in the mean curvature due to axial symmetry is $O(b/r)^{\frac{1}{2}}$ but numerical integration of the relevant equation shows that all these errors are slightly smaller than those contained in equation (35), which approach 10% when

$$(\rho gr^2/\sigma) - 0.842 = 0.25 \quad \text{and} \quad \mu U/\sigma = 8 \times 10^{-5}.$$

This estimate is for the error in the constants P , Q , R and hence in the profile attained by the meniscus well away from the wall. This profile is identified by the radius at which it would have a point of inflexion if it were continued outwards according to figure 7(a). Although the second term in equation (42) is $O(b/r)^{\frac{1}{2}}$ smaller than the first it may still consistently be retained for it arises only in relating r_I to r , once r_I has been correctly identified. Its omission would severely restrict the range of validity of the result.

4.3. *Experimental results*

Complete verification of equation (42) and of the prediction that the bubble will not rise is difficult. One requires, for any given fluid, a tube of constant diameter accurately known and very near the critical value. By chance, however, for water at 20°C and a tube of diameter 0.50 cm (nominal) $\rho gr^2/\sigma = 0.842$. The predicted rate of rise at 40°C is 2.1×10^{-3} cm/sec. The author immersed such a vertical tube in a water bath with temperature variable between 15 and 40°C. The results were not completely reproducible. At 15°C, $\rho gr^2/\sigma = 0.834$, the bubble was usually stationary; at 40°C it was always rising with speeds of the order of a few cm per hour. These speeds depended on the position in the tube and on whether it was accurately vertical. In view of the probable presence of impurities and of variations in the diameter of the tube, these results indicate quantitative agreement with the main conclusion that the bubble will not rise if $\rho gr^2/\sigma < 0.842$ and qualitative agreement with equation (42).

5. Conclusion

The theories of this paper form a small contribution to the problem of predicting the profile of a bubble in a capillary tube and the rate of rise of a bubble in a vertical tube. They are limited by the basic physical assumptions made about the properties of the free surface of liquid films under these conditions, that there should be a well-defined surface tension and hence no tangential stress on the surface. Perfect wetting on the tube wall is also essential. But provided inertia forces are negligible, and provided the film left on the wall during the passage of the bubble is sufficiently thin, the effects of viscous forces on the profile of the interface can be described by the lubrication equations, and are confined to a region near the wall. The remainder of the profile is governed by the same relations as if the bubble is stationary, but there is an intermediate region in which the two solutions can be matched. The thickness of fluid left on the wall is in each case determined uniquely by conditions at the front meniscus, whereas at the rear meniscus there is a steady solution matching smoothly onto any film thickness that should previously have been left there. At the rear meniscus also, the profile shows oscillations in thickness in advance of the main curvature. In a capillary tube the bubble moves slightly faster than the mean speed of the fluid in the tube, the fractional correction being $1.29(3\mu U/\sigma)^{\frac{1}{2}}$. At the slowest speeds the main pressure drop in such a tube arises from the slight difference in curvature between the front and rear menisci of the bubble, and is $4.52(\sigma/r)(3\mu U/\sigma)^{\frac{1}{2}}$. These results are only valid if $\mu U/\sigma < 5 \times 10^{-3}$.

The free rise of a long bubble in a vertical sealed tube is completely inhibited if $\rho gr^2/\sigma < 0.842$. This is associated with the existence of a profile in static equilibrium making zero angle of contact with the wall only for smaller radii. For radii up to 12% larger than the critical the rate of rise increases very rapidly, being given by

$$(\rho gr^2/\sigma) - 0.842 = 1.25(\mu U/\sigma)^{\frac{2}{3}} + 2.24(\mu U/\sigma)^{\frac{1}{2}}.$$

From a practical point of view the cases of most interest are when $\mu U/\sigma$ is larger than the very small values discussed here. When surface tension is not dominant, however, none of these methods are appropriate, and a satisfactory method of analysis has yet to be found.

The waves near the rear meniscus predicted in §2.2 are easily observable at larger film thicknesses than those for which theory is valid, and seem to be of quite general occurrence. From the point of view of causality, it is of interest that the values of b/r obtained are in each case determined by consideration of the front meniscus alone. The predictions of the pressure drop across the bubble in a capillary are also of no great practical use, for at the very small values of $\mu U/\sigma$ for which they apply, effects due to the variations in the radius of the tube are likely to be larger. The two-dimensional version of this theory is applicable to the motion of fingers in Hele-Shaw cells considered by Saffman & Taylor (1958), but the restriction to small values of $\mu U/\sigma$ precludes at present an explanation of their results. Experimental verification of this theory is unsatisfactory. For values of $\mu U/\sigma$ larger than 3×10^{-3} the results of this present work, those of Fairbrother & Stubbs (1935), Taylor (1961), and Goldsmith & Mason (1960) are in broad agreement that Fairbrother & Stubbs's formula $1.0(\mu U/\sigma)^{\frac{1}{2}}$ is a good estimate for the value of W up to $\mu U/\sigma = 0.08$, above which it over estimates the true value. Below 3×10^{-3} , which is also the upper limit of the present theory, there is widespread disagreement, and at the very slowest speeds the divergences between experiment and the two-thirds power law involve a factor of 8. Although in principle the method used by the present author is probably the most accurate in this range, he is unable even to suggest an explanation of this situation. There have also been widely differing estimates of the critical radius below which a long bubble in a vertical tube will not rise. This is surprising, for the phenomenon is striking, and above the critical point the speed of rise increases very rapidly with radius. Provided that adequate precautions are taken about cleanliness, that the cross-section of the tube be circular, and that it be accurately vertical, it should be possible in further experiments to narrow this range considerably.

The author is indebted to Sir Geoffrey Taylor and Dr P. G. Saffman for invaluable help and discussions, to Mr R. G. Wooding and Mr W. E. Thompson for assistance with experiments, to Dr S. G. Mason for commenting on this manuscript, and to the Department of Scientific and Industrial Research for a grant.

REFERENCES

- BARR, G. 1926 *Phil Mag.* **1**, 395.
 BASHFORTH, F. & ADAMS, J. C. 1883 *An Attempt to Test the Theories of Capillary Action*.
 Cambridge University Press.
 CHRISTOPHERSON, D. G. & DOWSON, D. 1959 *Proc. Roy. Soc. A*, **251**, 550.

- FAIRBROTHER, F. & STUBBS, A. E. 1935 *J. Chem. Soc.* **1**, 527.
- FORDHAM, S. 1948 *Proc. Roy. Soc. A* **194**, 1.
- FRENKEL, J. 1946 *Kinetic Theory of Liquids*, p. 332. Oxford University Press.
- FRUMKIN, A. & LEVICH, V. 1947 *Zh. fiz. khim. (J. Phys. Chem., Moscow)*, **21**, 1183.
- GIBSON, A. H. 1913 *Phil. Mag.* **26**, 952.
- GOLDSMITH, H. L. & MASON, S. G. 1960 Private Communication. McGill University, Montreal.
- MARCHESSAULT, R. N. & MASON, S. G. 1960 *Ind. Engng Chem.* **52**, 79.
- SAFFMAN, P. G. & TAYLOR, G. I. 1958 *Proc. Roy. Soc. A*, **245**, 312.
- TAYLOR, G. I. 1961 *J. Fluid Mech.* **10**, 161.